

Selective Equatorial Sclera Crosslinking in the Orbit Using a Metal-Coated Polymer Waveguide

Sheldon J. J. Kwok,^{1,2} Sarah Forward,¹ Christian M. Wertheimer,¹ Andreas C. Liapis,¹ Harvey H. Lin,¹ Moonseok Kim,¹ Theo G. Seiler,^{1,3,4} Reginald Birngruber,^{1,5} Irene E. Kochevar,¹ Theo Seiler,³ and Seok-Hyun Yun^{1,2}

¹Harvard Medical School and Wellman Center for Photomedicine, Massachusetts General Hospital, Boston, Massachusetts, United States

²Harvard-MIT Health Sciences and Technology, Massachusetts Institute of Technology, Cambridge, Massachusetts, United States

³Institute for Refractive and Ophthalmic Surgery (IROC), Zurich, Switzerland.

⁴Universitätsklinik für Augenheilkunde, Inselspital, Universität Bern, Bern, Switzerland

⁵Institut für Biomedizinische Optik, Universität zu Lübeck, Lübeck, Germany

Correspondence: Seok-Hyun Yun, Harvard University, 65 Landsdowne St. UP-525, Cambridge, MA 02139, USA; syun@hms.harvard.edu.

SJK and SF contributed equally to the work presented here and should therefore be regarded as equivalent authors.

Submitted: January 22, 2019

Accepted: May 15, 2019

Citation: Kwok SJJ, Forward S, Wertheimer CM, et al. Selective equatorial sclera crosslinking in the orbit using a metal-coated polymer waveguide. *Invest Ophthalmol Vis Sci*. 2019;60:2563-2570. <https://doi.org/10.1167/iovs.19-26709>

PURPOSE. Photochemical crosslinking of the sclera is an emerging technique that may prevent excessive eye elongation in pathologic myopia by stiffening the scleral tissue. To overcome the challenge of uniform light delivery in an anatomically restricted space, we previously introduced the use of flexible polymer waveguides. We presently demonstrate advanced waveguides that are optimized to deliver light selectively to equatorial sclera in the intact orbit.

METHODS. Our waveguides consist of a polydimethylsiloxane cladding and a polyurethane core, coupled to an optical fiber. A reflective silver coating deposited on the top and side surfaces of the waveguide prevents light leakage to nontarget, periorbital tissue. Postmortem rabbits were used to test the feasibility of in situ equatorial sclera crosslinking. Tensometry measurements were performed on ex vivo rabbit eyes to confirm a biomechanical stiffening effect.

RESULTS. Metal-coated waveguides enabled efficient light delivery to the entire circumference of the equatorial sclera with minimal light leakage to the periorbital tissues. Blue light was delivered to the intact orbit with a coefficient of variation in intensity of 22%, resulting in a $45 \pm 11\%$ bleaching of riboflavin fluorescence. A 2-fold increase in the Young's modulus at 5% strain (increase of 92% $P < 0.05$, at 25 J/cm^2) was achieved for ex vivo crosslinked eyes.

CONCLUSIONS. Flexible polymer waveguides with reflective, biocompatible surfaces are useful for sclera crosslinking to achieve targeted light delivery. We anticipate that our demonstrated procedure will be applicable to sclera crosslinking in live animal models and, potentially, humans in vivo.

Keywords: sclera, waveguide, crosslinking, myopia

Despite the rapidly increasing prevalence of myopia worldwide, interventions to control myopia progression have been inadequate. Of particular concern are patients with high myopia, who have an increased risk for potentially sight-threatening diseases, such as glaucoma and retinal detachment.¹ Various therapeutic modalities have been tested to halt myopic progression and prevent these complications.^{2,3}

The sclera has an important role in the development and progression of myopia.^{4,5} Scleral remodeling in myopia includes scleral thinning, loss of scleral tissue, weakening of the scleral mechanical properties and, ultimately, development of posterior staphyloma.⁶ This has led to the development of scleral collagen crosslinking (SXL) with light-activated photosensitizers to mechanically reinforce the scleral tissue and prevent subsequent changes in axial length.⁷⁻¹⁶ Corneal collagen crosslinking with light-activated photosensitizers currently is used clinically to treat patients with corneal ectatic disorders.^{17,18} However, significant technical challenges prevent clinical translation of SXL for myopia control. Compared to the

cornea, the sclera cannot be irradiated easily using an external light source. In designing a light-delivery apparatus to deliver light in the orbit, selective and uniform illumination also are critical requirements.^{16,19-22}

SXL using riboflavin in conjunction with ultraviolet A (UVA) or blue light has shown efficacy in reducing axial length elongation in several animal models of myopia,⁷⁻⁹ primarily targeting the scleral equator. Although protrusion of the posterior sclera is a hallmark of severe pathologic myopia,⁶ and while the whole sclera and cornea also show pathognomonic changes in myopia progression,⁴ targeting the equator has several advantages. The equator is relatively easy to access surgically, and furthermore, any potential photochemical toxicity would not be as severe as it would be at the posterior pole or the limbus, where nearby essential anatomic structures can be irreversibly damaged.

To target the equatorial region, fiberoptic approaches have been used to target small, selected regions of the sclera^{7,9} ($< 20 \text{ mm}^2$). In another study, a dental blue light source was used to



contact the exposed sclera to irradiate a relatively larger area^{8,23} ($\sim 100 \text{ mm}^2$). Active devices, such as miniature light-emitting diodes (LEDs) also can be used but have several drawbacks, including limited irradiance, risk of thermal tissue damage, and poor flexibility.^{20,24} Recently, we introduced the use of thin and flexible polymer waveguides for light delivery to the sclera, and demonstrated SXL of equatorial sclera around the entire circumference ($\sim 400 \text{ mm}^2$) of an ex vivo porcine eyeball. Compared to other devices, our waveguides enable uniform light delivery to large areas of the sclera with shorter procedural times and reduced invasiveness.¹⁶

We described a novel waveguide design optimized for SXL in vivo. Our waveguides have two major advantages over previous approaches. First, we use a core-cladded structure to ensure efficient light propagation irrespective of the surrounding environment, enabling light delivery inside the orbit while the waveguide is in contact with extraocular muscles, fluid, and other tissues. Second, a reflective metal coating deposited around the waveguide blocks light leakage from the outer surface of the waveguide, minimizing off-target irradiation to surrounding tissues, and decreasing risk of photochemical toxicity. The reflective coating also reduces optical loss in the waveguide when the waveguide is curved around the eyeball. As a proof of principle, we used our waveguides to irradiate equatorial sclera in a freshly excised rabbit head. We reported the surgical procedure to insert the waveguide into the orbit, and successfully demonstrated photobleaching of riboflavin around the eye. Finally, we confirmed stiffening of equatorial sclera with our technique on ex vivo rabbit eyes.

METHODS

Intended Use of Waveguides

Our waveguides were designed to be inserted into the Tenon's space underneath the rectus muscles within the orbit (Fig. 1). To enable insertion into such a tight anatomic space, we selected materials with high mechanical flexibility. For optimal light delivery, we also chose materials with high optical transparency. The optical design of the waveguide was optimized to deliver light from one side to scleral tissue, while minimizing light leakage to all other surfaces, preventing light exposure of extraocular muscles and other periorbital tissues. Light was coupled into the waveguide through a laser-coupled pigtail fiber, allowing convenient selection of wavelength and incident power.

Waveguide Fabrication

Polydimethylsiloxane (PDMS; Sylgard 184; Dow Corning, Midland, MI, USA) was prepared in a 10:1 volume ratio of elastomer to curing agent and poured into a square container with enough volume to result in a 0.5-mm thick layer. It was left to degas and cure at room temperature on a level surface for 48 hours. Next, a mixture of polyurethane (PU) elastomer (1:2 by weight of Clear Flex 50 precursors A:B; Smooth-On, Inc., Macungie, PA, USA) was prepared. The PU mixture was poured over the top of the PDMS, resulting in a 1-mm thick layer, and left at room temperature to cure for at least 16 hours. A second PDMS mixture was prepared as described previously and poured over the top of the PU with enough volume to result in a 0.25-mm thick layer. It was left to cure at room temperature for 48 hours. Next, the waveguide slab was cut into 4-mm wide strips with a commercial paper cutter (SmartCut Rotary Trimmer; Swingline, Lake Zurich, IL, USA). Once cut, the waveguides were turned onto their long edge and cladded with PDMS applied via a narrow syringe.

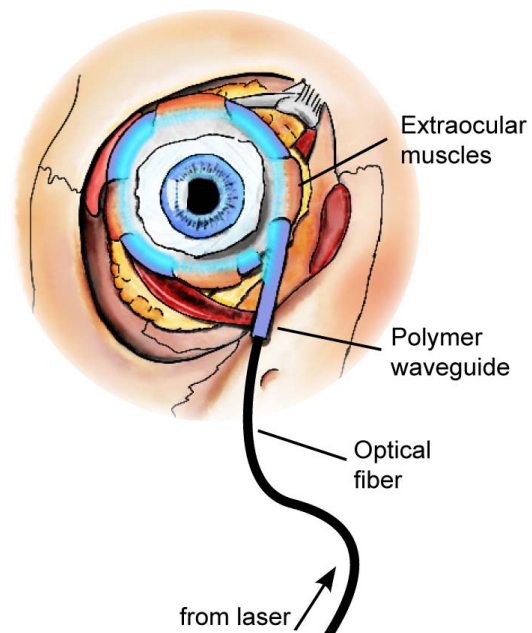


FIGURE 1. Schematic of a waveguide inserted in the orbit for crosslinking of equatorial sclera.

For metal coating, the polymer waveguides were mounted on a carrier wafer and placed in a sputter coater (208HR; Cressington, Watford, United Kingdom) such that the strips were off-angle with respect to the sputtering source. Eight sequential depositions of approximately 15 nm of silver were performed, manually varying the angle of the samples within the chamber after each one. As a result of this procedure, all sides other than the therapeutic side received a uniform coating of metal. To protect the silver deposition, a thin layer of $< 1 \text{ mm}$ PDMS was applied over the top. The PDMS outer layer ensures good biocompatibility with the tissue in contact.

To couple light into the waveguides, a 200 μm core ferrule patch cable (M95L01, 0.50 numerical aperture (NA), $\text{\O}1.25 \text{ mm}$, Thorlabs, Inc., Newton, NJ, USA) was connected to a 5 mm long, 200 μm core fiberoptic cannula (CFML52L05, 0.50 NA, $\text{\O}1.25 \text{ mm}$; Thorlabs, Inc.) via quick release interconnect (ADAL3; Thorlabs, Inc.). The cannula was inserted into the core on the short edge of the waveguide. A 30-gauge needle was used to perforate the core for easier insertion. Images of blue light coupled into the waveguide were taken from the top, bottom, and side to visualize the effect of the metal coating.

Tapered PDMS-only waveguides were fabricated for comparison following previously described procedures.¹¹ Briefly, a PDMS mixture was prepared in a 10:1 volume ratio of elastomer to curing agent in a square container placed on an incline to generate a 2.0 to 0.8 mm linearly tapered thickness along 7 cm. The mixture was cured at room temperature for 48 hours and cut into 4 mm strips with the same commercial paper cutter. These waveguides were coupled to the laser in the same fashion as the PU waveguides, via cannula, interconnect, and ferrule fiber.

Waveguide Design Parameters

To deliver light into the orbit, we distinguished between two distinct modes of light propagation within the waveguide. First, light propagation inside the straight section of the waveguide before it enters the orbit can be achieved through total internal reflection (TIR), with light rays alternately reflecting from the top and bottom core-cladding interfaces

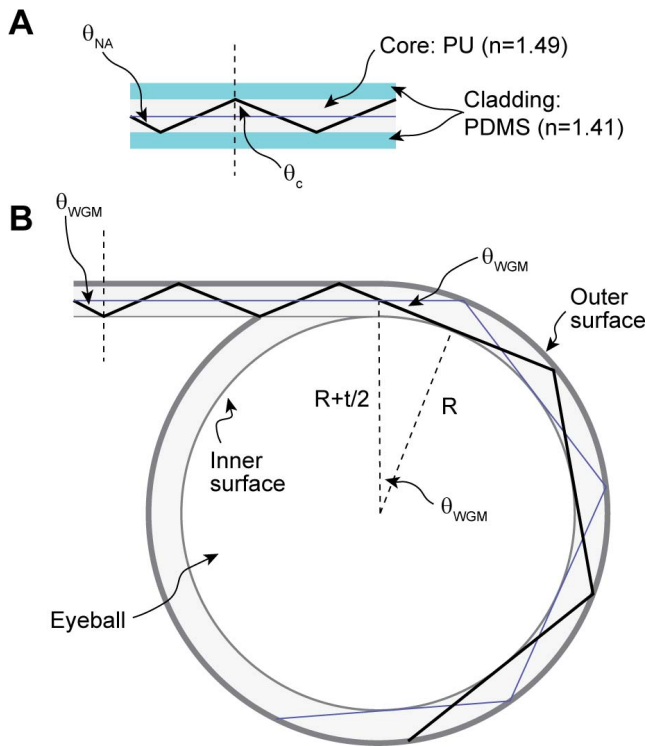


FIGURE 2. Two modes of light propagation within the waveguide. (A) Light propagates in the straight section through total internal reflection. (B) Light propagates in the curved section by reflecting only off the outer surface, known as WGM paths.

(Fig. 2A). The critical angle (θ_c) for TIR is:

$$\theta_c = \sin^{-1}\left(\frac{n_{cladding}}{n_{core}}\right) \quad (1)$$

where $n_{cladding}$ and n_{core} are the refractive indices of the cladding and the core of the waveguide, respectively. For an optical fiber inserted into the waveguide, the maximum incident angle defined by the incident fiber numerical aperture ($NA = n_{core}\sin\theta_{NA}$) should satisfy:

$$\theta_{NA} = \sin^{-1}\left(\frac{NA}{n_{core}}\right) = 90 - \theta_c \quad (2)$$

On the other hand, when the waveguide is wrapped around the eyeball, incoming light rays hit the outer surface of the waveguide (Fig. 2B). For light propagation inside the curved waveguide, the TIR condition does not hold for all incoming rays when periorbital tissues ($n \sim 1.4$) are in contact with the outer surface. Thus, high reflectivity of the outer surface is critical for uniform light delivery. With a reflecting surface, the optical rays follow so-called whispering gallery mode (WGM) paths, propagating by only reflecting off the outer surface of the waveguide. The full range of angles that satisfy the WGM guiding (θ_{WGM}) can be expressed by:

$$\theta_{WGM} = \cos^{-1}\left(\frac{R}{R+t/2}\right) \quad (3)$$

where R is the eyeball radius, and t is the waveguide thickness. Light is delivered to the underlying tissue through scattering loss, which depends on the roughness at the interfaces between the waveguide core and cladding, and between the cladding and outer surface. The scattering loss also may be increased by inserting bulk scatterers into the waveguide.

Light is coupled to the waveguide through a fiberoptic cannula, in which the cleaved end of an optical fiber (~ 5 mm) is inserted directly into the core of the waveguide (Fig. 3A). The NA of the input fiber was chosen to match both conditions for TIR in the straight geometry, and WGM propagation for the curved waveguide around the eyeball equator. For our waveguide materials, $\theta_c \approx 71^\circ$ using Equation 1. This corresponds to a $\theta_{NA} \approx 19^\circ$ using Equation 2, or $NA \leq 0.48$ to ensure that all incident rays in the straight geometry satisfy the TIR condition. For the curved geometry, the radius of the rabbit eyeball is 8 mm, the thickness of the waveguide core is 1 mm, and the top cladding thickness is 0.25 mm. Using Equation 3, $\theta_{WGM} \approx 22^\circ$, corresponding to a required $NA \leq 0.56$ for all incident rays to follow WGM-type paths around the eyeball. Our input fiber with $NA = 0.5$ performs adequately under these conditions.

Surgical Procedure for Waveguide Insertion

Fresh rabbit heads were obtained from animals that were sacrificed in another experimental protocol and used within 4

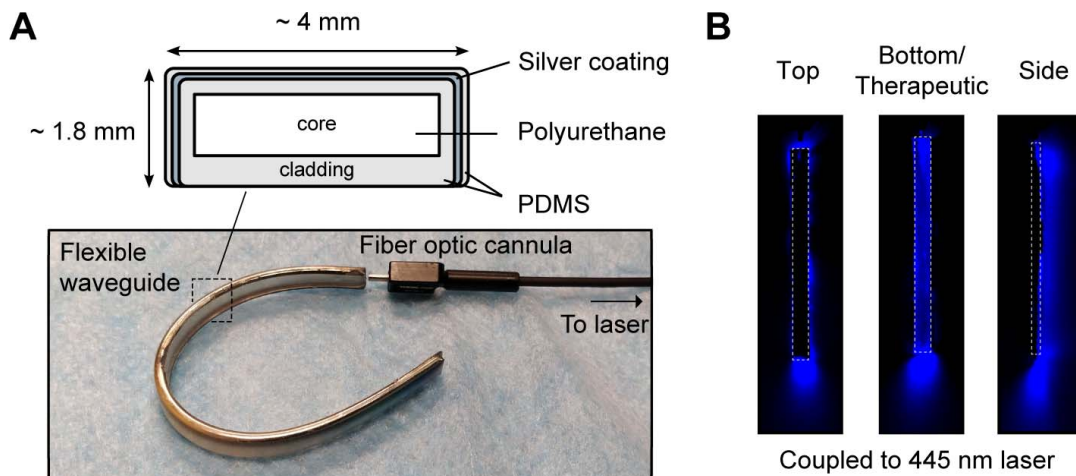


FIGURE 3. Waveguide device schematic. (A) Material composition and dimensions of our silver coated, PDMS-PU waveguides. Image showing our flexible waveguide, fiberoptic cannula, and input fiber. (B) Images of the top, bottom, and side of a waveguide (dotted white lines) with blue light coupled in through an input fiber.

hours of death. The Massachusetts General Hospital Institutional Animal Care and Use Committee (IACUC) approved the procedure (approval ID 2018N17), and all experiments comply with the ARVO Statement for the Use of Animals in Ophthalmic and Vision Research. After careful removal of the nictitating membrane a 360 degree limbal conjunctival peritomy was created by ophthalmic microscissors and the Tenon's capsule was removed from the sclera. The rectus ocular muscles were detected by a Graefe muscle hook, which was passed between the Tenon's capsule and sclera. Traction was placed on the hook towards the limbus to isolate the muscle, which then was marked by entwining with a 3-0 Prolene suture (Prolene, 3-0; Ethicon, Inc., Somerville, NJ, USA) to facilitate positioning the globe. The intermuscular fascia was pushed posteriorly with anatomic forceps. After marking all muscles, riboflavin (riboflavin 5'-monophosphate sodium salt, 0.5% wt/vol; Sigma-Aldrich Corp., St. Louis, MO, USA) was applied into the subconjunctival room and into the anterior periocular orbital region for 30 minutes, at which point a deep yellow color change of the sclera was apparent. The waveguide then was pushed below the muscles, which were gently pulled up to make room with the marking suture. This led to placement of the waveguide around the scleral equator within the orbit, inside the Tenon's space.

Light Delivery Profile

Light delivery profiles were recorded, before crosslinking, once the waveguide was positioned and coupled to a 445 nm continuous wave diode laser (LSR445CPD-4W; Lasever, Ningbo, China), set to low power (<1 mW). Images of the waveguide in situ were taken with a Nikon D90 camera (Nikon, Tokyo, Japan) alone, and through a 495 nm long pass filter (FGL495S; Thorlabs, Inc.) to collect the blue therapeutic light and green riboflavin fluorescence, respectively (Fig. 3A).

Photobleaching Quantification

Scleral crosslinking was performed using riboflavin and 445 nm blue light at a fluence of 44 J/cm². To prevent the eye from becoming dry throughout the duration of the crosslinking, a PBS-soaked tissue was placed over the eye. Afterward, the laser was turned off and the eye was excised from the orbit. After all muscles were carefully removed, the eye was positioned on a mount capable of 360-degree azimuthal rotation. Images were taken with white and blue light every 30° rotation of the eye. For blue light excitation, a blue bandpass filter (FF01-405/150-25 Brightline; Semrock, Inc., Rochester, NY, USA) was placed in front of a white light source, and images were taken through the 495 nm long pass filter. A negative control also was performed of an eye prepared in the same way as described, but without light coupled into the waveguide. Photobleaching was quantified as follows:

$$\text{Photobleaching} = 1 - \frac{Fl_{irr}}{Fl_{non-irr}} \quad (4)$$

where Fl_{irr} and $Fl_{non-irr}$ are the fluorescence intensities of the irradiated and nonirradiated regions, respectively.

Tensometry Measurements

Freshly frozen, mature, New Zealand White rabbit eyes (Pel-Freez Biologicals, Rogers, AR, USA) were slowly thawed in a moist chamber. The horizontal (nasal-temporal) orientation of the cornea was identified by the two horizontal scleral vortex vessels and marked on the limbal region using a surgical marker. To maintain equal hydration, the whole globe was placed in PBS (Fisher Bio Reagents, Fair Lawn, NJ, USA)

containing 20% wt/vol dextran (cat. no. 31392; MilliporeSigma, Burlington, MA, USA) for at least 30 minutes and stained in a 0.5% wt/vol riboflavin-PBS solution also containing 20% wt/vol dextran for another 30 minutes. The eye then was placed in a custom-made container to simulate the orbit and to keep the waveguide in place, which was wrapped around the eye along its equator. The equator and area of irradiation also were marked with the surgical marker.

For all irradiation procedures, a continuous-wave diode laser (LSR445CPD-4W; Lasever) emitting 445 nm (blue light) was used. The setup was calibrated by an optical power meter (PM400K2; Thorlabs, Inc.) before use to deliver an irradiance of approximately 7 mW/cm² through the waveguide to the equator. The irradiation time was set to 1 hour while the eye was kept in a moist environment. For each eye that was crosslinked, we prepared a no-light control with the same conditions, but with no light irradiation, and an untreated control. Ten eyes were used for each group.

After irradiation, two 5 mm scleral strips were cut from the previously marked horizontal (nasal-temporal) orientation using fixed distance-separated razor blades. The exact width was measured by a digital caliper (ABSOLUTE Digimatic 500-196-30; Mitutoyo, Takatsu-ku, Japan). The thickness of each strip was determined by a home-built optical coherence tomography (OCT) b-scan where the average of 32 slices was taken to be the average thickness of each strip of equatorial sclera. For the tensile strength measurements, the initial length was set to 3 mm and matched with the marked area from the irradiated equator. Force generated as a function of change in length was determined using a tensometer (eXpert 4000; Admet, Norwood, MA, USA), following a previously published procedure.¹⁶ The Young's modulus was calculated between 0.5% and 5% strain and stress-strain curves were plotted as a surrogate marker for crosslinking strength.

Statistics

To quantify light delivery and photobleaching profiles, we computed the coefficient of variation, which is defined as standard deviation divided by the mean. Data were analyzed in MATLAB (MathWorks, Inc., Natick, MA, USA). Statistical testing was performed in GraphPad Prism (GraphPad Software, San Diego, CA, USA). A 1-way ANOVA was used to analyze tensometry results. The Lilliefors test confirmed normal distribution of data for each group ($P > 0.05$). Posterior hoc analyses were conducted using Tukey's honestly significant difference (HSD) testing at the $\alpha = 0.05$ level.

RESULTS

Waveguide Design

Our waveguides have a core-cladded structure, in which PU is the higher refractive index core ($n = 1.49$), and PDMS is the lower refractive index cladding ($n = 1.41$; Fig. 3A). PU and PDMS are optically transparent in the visible wavelengths (transmittance > 90% per cm) and highly flexible (elongation at break > 100%). A thin layer of silver (< 200 nm, with reflectivity > 90%) is coated over the top and sides of the waveguide to ensure light delivery only from the therapeutic side of the waveguide (Fig. 3B). To prevent disruption of the metal layer, a final sealant layer of PDMS is coated around the entire waveguide. The typical dimensions of our waveguides were 70 × 4 × 1.8 mm. Light is coupled to the waveguide through a fiberoptic cannula, in which the cleaved end of the fiber (~ 5 mm) is inserted directly into the core of the waveguide. The cannula is connected to an optical patch cable

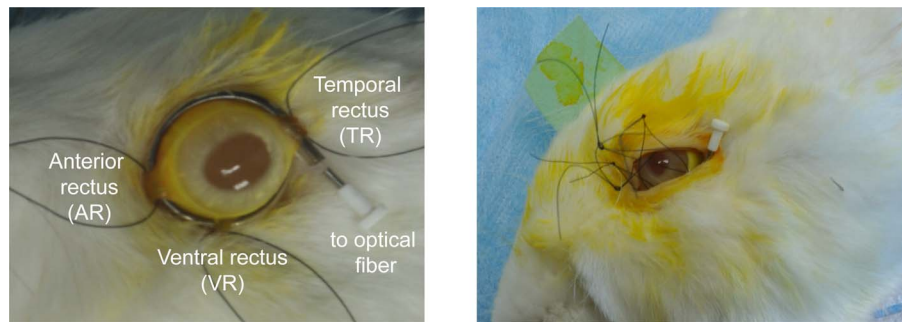


FIGURE 4. Images of the waveguide inserted in the intact orbit of a postmortem rabbit following staining with riboflavin. The waveguide is placed underneath the temporal rectus (TR), anterior rectus (AR), and ventral rectus (VR) muscles.

through a detachable fiber interconnect, which enables light to be coupled after the waveguide is securely in place around the eyeball. For SXL, we coupled blue light (445 nm) through the input fiber into the waveguide. To maximize light guiding efficiency and uniformity of light delivery, the NA of the input fiber (NA = 0.50) was chosen to match both conditions for total internal reflection in the straight geometry, and whispering gallery mode propagation for the curved waveguide around the eyeball equator (see Methods). Light is delivered to the underlying tissue through scattering loss from surface roughness and bulk scattering.

Light Delivery to Sclera in the Rabbit Head

To demonstrate feasibility of SXL using our waveguides, we chose to use a rabbit model due to similarities with human anatomy, particularly the presence and location of the extraocular muscles. Experiments were performed on freshly excised rabbit heads to simulate *in vivo* conditions. Following removal of the conjunctiva and application of riboflavin, our waveguides were safely and securely inserted beneath the rectus muscles. Of note, the small geometric footprint of our waveguides enable them to fit completely inside the orbital cavity (Fig. 4).

To characterize the uniformity of light delivery to the sclera inside the rabbit orbit, we coupled blue light into the waveguide (Fig. 5A). The green fluorescence of the riboflavin-stained sclera was used to quantify the amount of light delivered. Our metal-coated, core-cladded waveguides deliver light throughout the entire circumference of the equatorial

sclera, and is unaffected by the presence of muscles. In contrast, light delivery from the PDMS waveguide drops dramatically shortly after entering the orbit, reaching virtually no light after passing the anterior rectus muscle. Figure 5B shows the fluorescence intensity from where the waveguide was inserted proximally to the distal end of the waveguide, with regions blocked by the rectus muscles excluded. The coefficient of variation in the fluorescence profile was 22% for the metal-coated waveguides and 149% for the PDMS-only waveguides. Exponential fitting of the light delivery profile yielded a delivery length (defined as the length at which distal light delivery reaches 50% of proximal) of 53 ± 4 mm for the metal-coated waveguides and 5 ± 2 mm for the PDMS only waveguides.

Sclera Crosslinking

As a proof of principle for SXL, we first quantified photobleaching of riboflavin after irradiation of equatorial sclera in the rabbit head. Figure 6A shows images of the equatorial sclera before and after irradiation at a fluence of 0 and approximately 44 J/cm^2 using our metal-coated waveguides. A representative axial profile of the eyeball fluorescence comparing the intensity of the irradiated equatorial sclera to nonirradiated anterior and posterior sclera is shown in Figure 6B. The mean photobleaching efficacy measured around the equatorial circumference was $45\% \pm 11\%$, corresponding to a coefficient of variation of 24% (Fig. 6C).

To confirm that our method induces a biomechanical effect on the rabbit sclera, we performed SXL with our waveguides

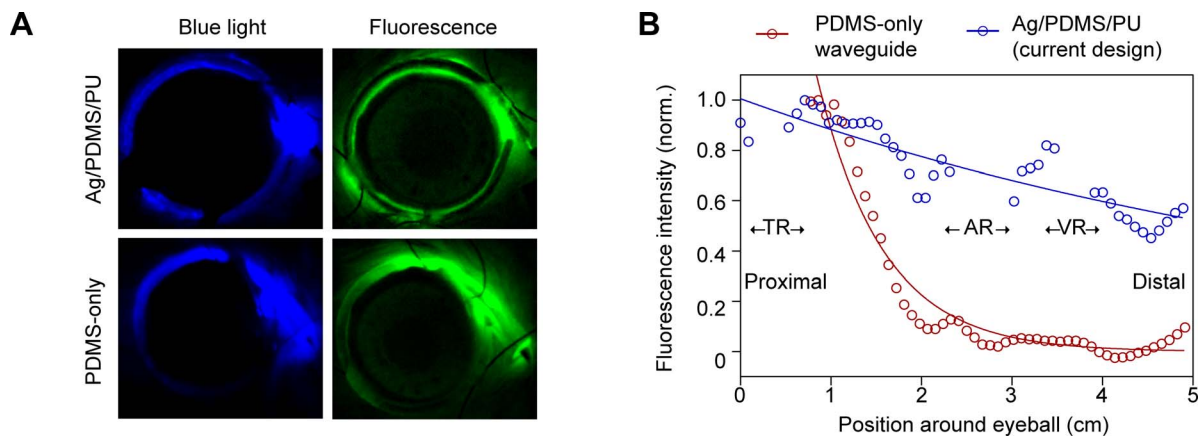


FIGURE 5. Uniformity of light delivery. (A) Images of the blue light and green fluorescence from light delivered to riboflavin-stained sclera in the intact orbit. Light delivery through Ag/PDMS/PU and PDMS-only waveguides were compared. (B) Light delivery profiles for the two types of waveguides. Data were excluded for regions blocked by ocular muscles. The location of the muscles is indicated in Figure 4.

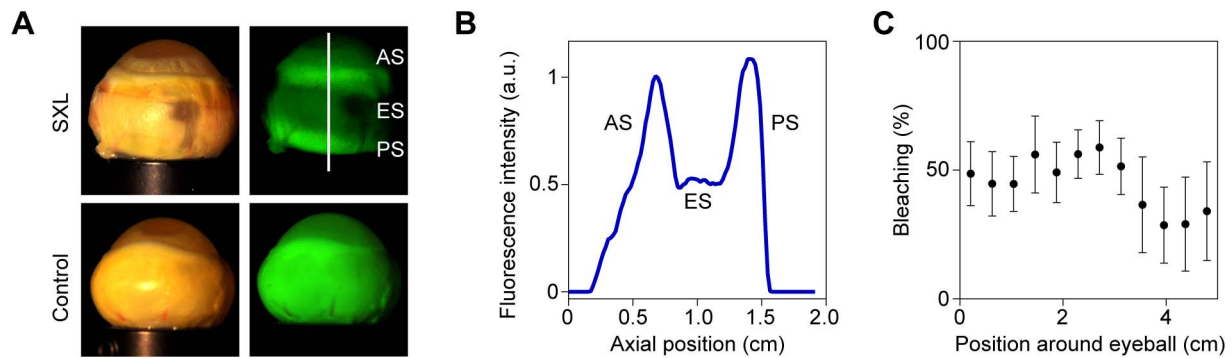


FIGURE 6. Quantification of riboflavin photobleaching. (A) Representative images of the enucleated eyeball following SXL in the orbit at 44 J/cm^2 , compared to a no-light control (0 J/cm^2). The muscles were removed for this analysis. AS, anterior sclera; ES, equatorial sclera; PS, posterior sclera. (B) Axial profile of riboflavin fluorescence intensity of the region indicated in Figure 5A. (C) Quantification of photobleaching around the eyeball following irradiation with our waveguides at 44 J/cm^2 . Bleaching percent is reported as mean \pm SD.

on enucleated rabbit eyes at a fluence of 0 and approximately 25 J/cm^2 and measured changes in the Young's modulus compared to untreated controls (Fig. 7). At 5% strain, the Young's modulus for samples irradiated with approximately 25 J/cm^2 was significantly higher than that of untreated controls (increase of 147%, $P = 0.009$), and significantly higher than that of no-light controls (increase of 92%, $P = 0.04$). We found no significant difference between untreated and no-light controls ($P = 0.81$), confirming the stiffening effect was due to the combination of light and photosensitizer.

DISCUSSION

Targeting scleral tissue in the orbital cavity is challenging due to the difficulty of accessing the tissue through relatively limited anatomic space (Fig. 1). Furthermore, the potential phototoxicity to surrounding tissues poses another challenge. Unintended crosslinking of the extraocular muscles could have damaging effects to eye movement, and irradiation of the limbal region may impair stem cell function.²⁵ In this study, we designed waveguides that deliver light selectively to the sclera, while sparing surrounding tissues. Our metal-coated waveguides efficiently blocked any light leaking through the outer surface and sides of the waveguide, only allowing light delivery from the bottom, therapeutic side in contact with the sclera

(Fig. 3B). Using our waveguides, we demonstrated successful riboflavin photobleaching of the equatorial sclera in the intact orbit (Fig. 6), and achieved a 2-fold increase in stiffness compared to no-light controls (Fig. 7).

PU and PDMS were chosen for fabrication of our waveguides due to their optical and material properties. The high optical transmittance of both materials minimizes absorption loss and prevents thermal damage due to heat generation. Furthermore, the refractive index contrast between the PU core ($n = 1.49$) and PDMS cladding ($n = 1.41$) allows for light guiding through TIR. In comparison, PDMS-only waveguides do not efficiently deliver light in the orbit (Fig. 5A) due to the similar refractive index of PDMS and surrounding tissues ($n = 1.33\text{--}1.4$). The small geometric footprint of our polymer waveguides, as well as their softness and high flexibility enable them to fit comfortably beneath the ocular muscles and completely in the orbit (Fig. 4), which avoids the need to maintain an artificial exophthalmos during the SXL procedure. To protect the thin silver coating, PDMS, a biocompatible material,²⁶ was used to encapsulate the entire waveguide. Repeated use of the waveguides in the rabbit head had no appreciable effect on the waveguide appearance or function.

A major advantage of our waveguide-based approach is the large therapeutic area. Using our metal-coated waveguides,

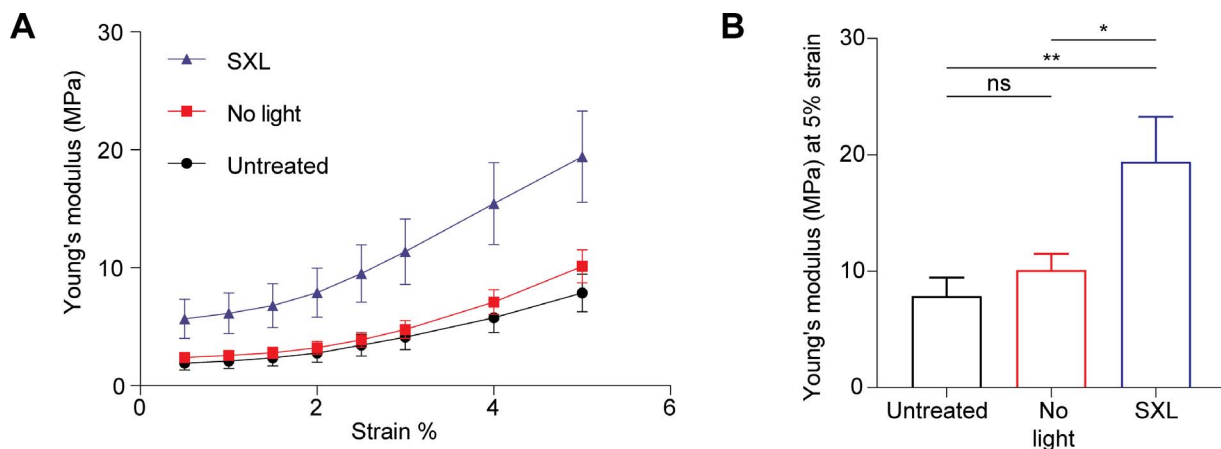


FIGURE 7. Tensometry measurements on enucleated rabbit eyes. (A) Young's modulus as a function of strain. SXL eyes were crosslinked at 25 J/cm^2 with our waveguides. No light samples (0 J/cm^2) were treated with the same conditions as SXL samples except with no light irradiation. Young's modulus is reported as mean \pm SE, with $N = 10$ eyes for each group. (B) Young's modulus reported at 5% strain comparing the stiffness of untreated, no light, and SXL-treated samples. SXL-treated samples were significantly different than untreated (1-way ANOVA $F[2, 27] = 5.69$, $P < 0.01$). Post hoc tests conducted with Tukey's HSD: ns (not significant); $*P < 0.05$; $**P < 0.01$.

light can be delivered simultaneously to the entire circumference of the equatorial sclera (Fig. 5). In contrast to previous approaches targeting multiple small regions of the sclera,^{7,9} our approach significantly reduces the SXL procedure time. The variation in light delivery using our metal-coated waveguides was approximately 22% (Fig. 5B), which was consistent with our photobleaching results (Fig. 6C). Higher uniformity of light delivery could be obtained by varying the scattering profile along the length of the waveguide, such as by tapering the thickness. Importantly, light irradiation with our metal-coated waveguides was limited to the equatorial sclera without affecting the anterior and posterior segments (Figs. 6A, 6B). This is in contrast to other techniques using unconstrained illumination that may indirectly expose the retina, which is particularly sensitive to blue light (ICNIRP exposure limit = 0.1 mW/cm² at 445 nm for 1 hour exposure time²⁷).

At a delivered fluence of 25 J/cm² to the sclera, we achieved a 2-fold increase in the Young's modulus at 5% strain (Fig. 7), which is comparable to other SXL studies.^{15,16} The fluence level used in our study is approximately one order of magnitude lower than previously measured damage thresholds for rabbit sclera (240–480 J/cm²).^{23,28} We used an irradiance level of 7 mW/cm², meaning at least 98% of the light irradiance must be directed away from the retina to prevent injury.²⁷ While the exact number is difficult to quantify, we note that light absorption (e.g., by riboflavin-stained tissue) likely precludes any appreciable amount of what little light has escaped through the waveguide coating (reflectivity > 90%) from reaching the retina. More efficient crosslinking at lower irradiances also may be possible in vivo due to higher oxygen availability, which also would further reduce treatment times.²⁹ In this study, we chose to target equatorial sclera primarily due to lower risk of phototoxicity compared to the posterior sclera. Further modifications to our waveguides also may enable targeting of the posterior sclera, to prevent thinning of the posterior pole and development of posterior staphyloma. Future studies in animal models and humans in vivo will test the efficacy and safety of our method for SXL.

Acknowledgments

The authors thank Bryan Mendes for tensometry measurements, Antoine Ramier for OCT measurements, Gregory Doerk and Chang-Yong Nam for metal coating of the waveguides, and Behrouz Tavakol, Soroush Shabahang, Seonghoon Kim, and Paul Dannenberg for useful discussions.

Supported by National Institutes of Health (Bethesda, MD, USA) Grants R01-EY025454, R41EY028820, and P41-EB015903, and the U.S. Air Force Office of Scientific Research (FA9550-17-1-0277). This research used resources of the Center for Functional Nanomaterials, which is a U.S. DOE Office of Science Facility, at Brookhaven National Laboratory under Contract No. DE-SC0012704.

Disclosure: S.J.J. Kwok, P; S. Forward, None; C.M. Wertheimer, None; A.C. Liapis, None; H.H. Lin, None; M. Kim, P; T.G. Seiler, None; R. Birngruber, None; I.E. Kochevar, None; T. Seiler, None; S.-H. Yun, P

References

- World Health Organization. *The Impact of Myopia and High Myopia*. 2015. Available at: <https://www.who.int/blindness/causes/MyopiaReportforWeb.pdf>.
- Cheng D, Schmid KL, Woo GC, et al. Randomized trial of effect of bifocal and prismatic bifocal spectacles on myopic progression: two-year results. *Arch Ophthalmol*. 2010;128:12–19.
- Tong L, Huang XL, Koh AL, et al. Atropine for the treatment of childhood myopia: effect on myopia progression after cessation of atropine. *Ophthalmology*. 2009;116:572–579.
- McBrien NA, Gentle A. Role of the sclera in the development and pathological complications of myopia. *Prog Retin Eye Res*. 2003;22:307–338.
- Funata M, Tokoro T. Scleral change in experimentally myopic monkeys. *Graefes Arch Clin Exp Ophthalmol*. 1990;228:174–179.
- Liu KR, Chen MS, Ko LS. Electron microscopic studies of the scleral collagen fiber in excessively high myopia. *Taiwan Yi Xue Hui Za Zhi*. 1986;85:1032–1038.
- Liu S, Li S, Wang B, et al. Scleral cross-linking using riboflavin UVA irradiation for the prevention of myopia progression in a guinea pig model: blocked axial extension and altered scleral microstructure. *PLoS One*. 2016;11:e0165792.
- Iseli HP, Körber N, Koch C, et al. Scleral cross-linking by riboflavin and blue light application in young rabbits: damage threshold and eye growth inhibition. *Graefes Arch Clin Exp Ophthalmol*. 2016;254:109–122.
- Dotan A, Kremer I, Livnat T, Zigler A, Weinberger D, Bouria. Scleral cross-linking using riboflavin and ultraviolet-A radiation for prevention of progressive myopia in a rabbit model. *Exp Eye Res*. 2014;127:190–195.
- Wollensak G, Iomdina E. Long-term biomechanical properties of rabbit sclera after collagen crosslinking using riboflavin and ultraviolet A (UVA). *Acta Ophthalmol*. 2009;87:193–198.
- Iseli HP, Spoerl E, Wiedemann P, Krueger R, Seiler T. Efficacy and safety of blue-light scleral cross-linking. *J Refract Surg*. 2008;24:S752–S755.
- Dotan A, Kremer I, Gal-Or O, et al. Scleral cross-linking using riboflavin and ultraviolet-A radiation for prevention of axial myopia in a rabbit model. *J Vis Exp*. 2016;110:e53201.
- Wang M, Corpuz CCC. Effects of scleral cross-linking using genipin on the process of form-deprivation myopia in the guinea pig: A randomized controlled experimental study. *BMC Ophthalmol*. 2015;15:89.
- Chu Y, Cheng Z, Liu J, Wang Y, Guo H, Han Q. The effects of scleral collagen cross-linking using glyceraldehyde on the progression of form-deprived myopia in guinea pigs. *J Ophthalmol*. 2016;2016:3526153.
- Zhang Y, Li Z, Liu L, Han X, Zhao X, Mu G. Comparison of riboflavin/ultraviolet-A cross-linking in porcine, rabbit, and human sclera. *Biomed Res Int*. 2014;2014:194204.
- Kwok SJJ, Kim M, Lin HH, et al. Flexible optical waveguides for uniform periscleral cross-linking. *Invest Ophthalmol Vis Sci*. 2017;58:2596–2602.
- Hersh PS, Stulting RD, Muller D, Durrie DS, Rajpal RK; U.S. Crosslinking Study Group. U.S. Multicenter Clinical Trial of Corneal Collagen Crosslinking for Treatment of Corneal Ectasia after Refractive Surgery. *Ophthalmology*. 2017;124:1475–1484.
- Raiskup-Wolf F, Hoyer A, Spoerl E, Pillunat LE. Collagen crosslinking with riboflavin and ultraviolet-A light in keratoconus: long-term results. *J Cataract Refract Surg*. 2008;34:796–801.
- Elsheikh A, Phillips JR. Is scleral cross-linking a feasible treatment for myopia control? *Ophthalmic Physiol Opt*. 2013;33:385–389.
- Hafezi For, Richoz O. Scleral CXL to treat progressive myopia. *Cataract Refract Surg Today Eur*. 2015;1–2.
- Raff AB, Seiler TG, Apiou-Sbirlea G. Bridging medicine and biomedical technology: enhance translation of fundamental research to patient care. *Biomed Opt Express*. 2017;8:5368–5373.
- Shabahang S, Kim S, Yun SH. Light-guiding biomaterials for biomedical applications. *Adv Funct Mater*. 2018;28:1706635.

23. Iseli HP, Körber N, Karl A, et al. Damage threshold in adult rabbit eyes after scleral cross-linking by riboflavin/blue light application. *Exp Eye Res.* 2015;139:37-47.
24. Xiao B, Chu Y, Wang H, Han Q. Minimally invasive repetitive UVA irradiation along with riboflavin treatment increased the strength of sclera collagen cross-linking. *J Ophthalmol.* 2017; 2017:1-6.
25. Moore JE, Schirotti D, Moore CBT. Potential effects of corneal cross-linking upon the limbus. *Biomed Res Int.* 2016;2016: 5062064.
26. Park G, Chung HJ, Kim K, Lim SA, et al. Immunologic and tissue biocompatibility of flexible/stretchable electronics and optoelectronics. *Adv Healthc Mater.* 2014;3:515-525.
27. International Commission on Non-Ionizing Radiation Protection. Guidelines on the limits of exposure to laser radiation of wavelengths between 180 nm and 1,000 μm . *Health Physics.* 1996;71:804-819.
28. Karl A, Makarov FN, Koch C, et al. The ultrastructure of rabbit sclera after scleral crosslinking with riboflavin and blue light of different intensities. *Graefes Arch Clin Exp Ophthalmol.* 2016;254:1567-1577.
29. Richoz O, Hammer A, Tabibian D, Gatziofuz Z, Hafezi F. The biomechanical effect of corneal collagen cross-linking (CXL) with riboflavin and UV-A is oxygen dependent. *Trans Vis Sci Tech.* 2013;2(7):6.